

Arabidopsis Stomatal Initiation Is Controlled by MAPK-Mediated Regulation of the bHLH SPEECHLESS

Gregory R. Lampard,* Cora A. MacAlister,* Dominique C. Bergmann†

Stomata, epidermal structures that modulate gas exchange between plants and the atmosphere, play critical roles in primary productivity and the global climate. Positively acting transcription factors and negatively acting mitogen-activated protein kinase (MAPK) signaling control stomatal development in *Arabidopsis*; however, it is not known how the opposing activities of these regulators are integrated. We found that a unique domain in a basic helix-loop-helix (bHLH) stomatal initiating factor, SPEECHLESS, renders it a MAPK phosphorylation target in vitro and modulates its function in vivo. MAPK cascades modulate a diverse set of activities including development, cell proliferation, and response to external stresses. The coupling of MAPK signaling to SPEECHLESS activity provides cell type specificity for MAPK output while allowing the integration of multiple developmental and environmental signals into the production and spacing of stomata.

In *Arabidopsis*, stomatal fate and pattern are regulated by three closely related basic helix-loop-helix (bHLH) transcription factors—SPEECHLESS (SPCH), MUTE, and FAMA—that, in partnership with the more distantly related bHLHs ICE1/SCREAM and SCREAM2, control initiation of asymmetric divisions, proliferation of transient precursor cells, and differentiation of stomatal guard cells, respectively (fig. S1) (1–4). Acting in opposition to these stomatal promoting factors are signaling systems that limit stomatal density and establish pattern. These negative regulators include the ERECTA (ER) family of leucine-rich repeat (LRR) receptor-like kinases (5, 6) and the LRR receptor-like protein TOO MANY MOUTHS (TMM) (7) that both may work in concert with the putative ligand EPF1 (8). A subtilisin protease, SDD1, also negatively regulates stomatal production but may act independently of this receptor-ligand module (8, 9).

Genetic evidence places a mitogen-activated protein kinase (MAPK) signaling cascade downstream of the receptors in stomatal development (10, 11). In all eukaryotes, MAPK cascades control a diverse array of activities, including the regulation of cell division and differentiation and the coordination of responses to environmental inputs (12, 13). The MAPK components implicated in stomatal development (YODA, MKK4/5, and MPK3/6) are broadly expressed (11, 14) and are involved in multiple activities. For example, YODA is required for asymmetric cell divisions in the embryo (15), and MKK4/5 and MPK3/6 were initially characterized by their roles in stress and pathogen responses (16, 17). Because of these multiple roles, a major challenge in MAPK signaling is to understand how common signaling elements evoke specific responses. Spatially or

temporally restricted expression of MAPK substrates could provide this specificity. Developmental MAPK substrates have not been previously described in plants; however, the cell type-specific expression and activities of SPCH, MUTE, and FAMA make these proteins attractive candidates for such specificity factors. Here we show that SPCH is a substrate of MPK3 and MPK6 in vitro, that specific phosphorylation sites on SPCH regulate its activity in vivo, and that known components of the stomatal development signaling network modulate SPCH behavior.

The *SPCH* loss-of-function phenotype is strikingly similar to that caused by constitutive activa-

tion of the MAPK pathway components YODA and MKK4/5 (10, 11), and *spch* is epistatic to *yoda* (2); these results are consistent with SPCH being a downstream target of MAPKs in the epidermis. To test whether SPCH is regulated by MAPK activity, we examined the expression of transcriptional (*SPCHpro::GFP*) and translational (*SPCHpro::SPCH-GFP*) reporters (GFP, green fluorescent protein) in plants expressing constitutively active (CA) YODA (*YODApr::CA-YODA*) (11). At 5 days post-germination (dpg), both wild-type plants (20 of 20) and *YODApr::CA-YODA* plants (19 of 20) expressed *SPCHpro::GFP* (fig. S2, A and B). Wild-type plants also expressed *SPCHpro::SPCH-GFP* (20 of 20), but *YODApr::CA-YODA* plants did not (0 of 20; fig. S2, C and D); this result suggests that YODA does not prevent transcription of *SPCH*, but rather limits the production or abundance of SPCH protein.

Phosphorylation of transcription factors can modulate their levels and activities (18, 19). We tested whether SPCH was an in vitro substrate for phosphorylation by the MAPKs previously implicated in stomatal development (MPK3 and MPK6) (10). SPCH, but not its paralogs FAMA and MUTE, could be phosphorylated by both MPK3 and MPK6 (Fig. 1B and fig. S3A). Alignment of SPCH, MUTE, and FAMA proteins reveals high sequence conservation in their bHLH domains and C termini (Fig. 1A) (2). However, SPCH also has a unique 93-amino acid domain [herein referred to as the MAPK target domain (MPKTD)] that contains 10 consensus MAPK phosphorylation target sites. Five of these sites

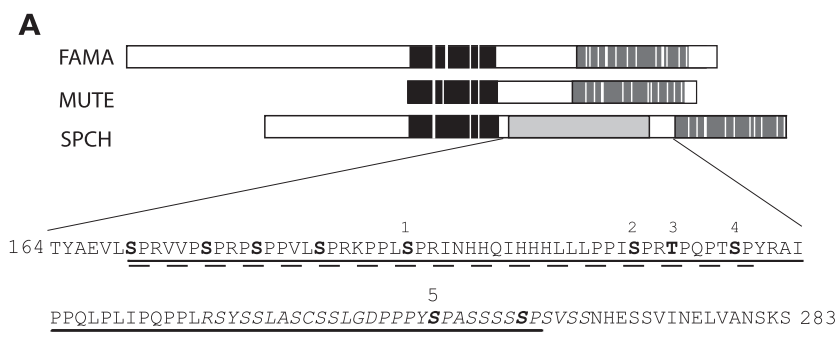
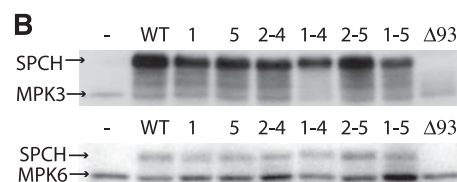


Fig. 1. SPCH is a stomatal regulator that contains a unique MAPK phosphorylation target domain. **(A)** Protein alignment of SPCH, MUTE, and FAMA. Highest conservation is in the bHLH domain (black) and C terminus (dark gray). White lines within these domains indicate nonidentical residues. The sequence of the MPKTD is shown with beginning and ending amino acid residue positions. Deletions are denoted as a solid underline for $\Delta 93$, a long-dashed underline for $\Delta 49$, and a short-dashed underline for $\Delta 31$. Italics denote the predicted PEST sequence. MAPK target sites are in bold. High-stringency sites are denoted 1 (Ser¹⁹³), 2 (Ser²¹¹), 3 (Thr²¹⁴), 4 (Ser²¹⁹), and 5 (Ser²⁵⁵). Abbreviations for amino acid residues: A, Ala; C, Cys; D, Asp; E, Glu; G, Gly; H, His; I, Ile; K, Lys; L, Leu; N, Asn; P, Pro; Q, Gln; R, Arg; S, Ser; T, Thr; V, Val; Y, Tyr. **(B)** In vitro activity of recombinant MPK3 (top) and MPK6 (bottom) on bacterially expressed SPCH variants. Lane labels indicate specific SPCH variant tested. Arrows correspond to phosphorylated SPCH and autophosphorylation of MPKs.



Department of Biology, Stanford University, Stanford, CA 94305, USA.

*These authors contributed equally to this work.

†To whom correspondence should be addressed. E-mail: dbergmann@stanford.edu

contain a Pro-X-Ser/Thr-Pro (P-X-S/T-P) motif, marking them as high-stringency sites (20) (Fig. 1A). Because SPCH differs from the nonsubstrate MUTE and FAMA proteins primarily in the MPKTD, we performed phosphorylation assays with a version of SPCH lacking the MPKTD and with the MPKTD alone. All MPK3 and MPK6 *in vitro* phosphorylation target sites appear to be contained within the SPCH MPKTD (Fig. 1B and fig. S3).

We then tested the functional importance of the SPCH MPKTD by using both the strong, broadly expressed 35S promoter and the endogenous SPCH promoter to express full-length SPCH and SPCHΔMPKTD variants in plants. Expression of 35S::SPCH was previously reported to induce divisions in pavement cells (2) and to produce extra stomatal lineage cells (3). 35S::SPCH expression in wild-type plants resulted in additional

divisions in pavement cells and a modest increase in total epidermal cell number (Fig. 2B), whereas expression of SPCH_{pro}::SPCH in the wild type resulted in no significant phenotypic effects (Fig. 3). In contrast to these results with full-length SPCH, SPCHΔMPKTD variants markedly affected epidermal development. When the entire domain was deleted (35S::SPCHΔ93 or SPCH_{pro}::SPCHΔ93), the epidermis of transformed plants exhibited large clusters of stomata (Fig. 2C and fig. S4), a phenotype similar to that produced by 35S::MUTE (2, 3). The SPCHΔ93 results are unsurprising given the strong similarity of SPCH and MUTE—particularly when the MPKTD is removed (Fig. 1A)—and in light of previous reports that overexpression of FAMA deletion variants mimics 35S::MUTE (1).

More informative were the phenotypes induced by expressing a smaller deletion that eliminates

eight target sites (four of five high-stringency sites) but leaves the fifth high-stringency site (Ser²⁵⁵) intact (SPCHΔ49, Fig. 1A) or the complementary deletion that removes the remaining target sites (SPCHΔ31, Fig. 1A). Expression of each deletion variant produced excessive numbers of asymmetric cell divisions in the epidermis, with SPCHΔ49 producing a stronger but qualitatively similar phenotype to that of SPCHΔ31 when expressed with the same promoter (Fig. 2D and fig. S4, B to D). The divisions induced by SPCHΔ49 and SPCHΔ31 were physically asymmetric and created cells with meristemoid morphology, much like the stomatal lineage—establishing divisions that SPCH promotes during normal development. To better characterize the cells produced by ectopic divisions, we monitored the expression of cell fate markers. Nearly all small, ectopic cells expressed *TMM*_{pro}::*TMM*-GFP, a general marker of cells in the stomatal lineage (Fig. 2, E and F) (7). A smaller fraction expressed *MUTE*_{pro}::GFP, a marker that is normally expressed in meristemoids just before their transition to guard mother cells (GMCs) (2). Thus, the population evidently consists of both meristemoids and other stomatal lineage cells (fig. S4H).

The division-promoting behavior of both SPCHΔ49 and SPCHΔ31 suggests that multiple residues within the MPKTD are functionally important. To define the specific residues, we repeated the *in vitro* and *in vivo* assays with SPCH variants in which the phosphorylatable S/Ts of the five high-stringency phosphorylation sites were substituted with nonphosphorylatable alanines. Each of these S/T → A variants was made as a fusion protein with yellow fluorescent protein (YFP) at the C terminus and was expressed with the SPCH promoter (21). Converting all five high-stringency MAPK target residues to alanines (SPCH_{pro}::SPCH1-5 S/T>A) resulted in a protein that created ectopic stomata like those created by SPCH_{pro}::SPCHΔ93 (Fig. 2G). Converting the first four sites to alanines (SPCH_{pro}::SPCH1-4 S/T>A) resulted in ectopic division phenotypes similar to those seen with SPCH_{pro}::SPCHΔ49 (Fig. 2H). The effect of SPCH_{pro}::SPCH5 S/T>A, however, was much weaker than that of SPCH_{pro}::SPCHΔ31 (Fig. 3 and fig. S4, D and E).

To test whether specific S/T residues or the overall number of S/T sites were important for SPCH regulation, we made additional combinations of S/T → A changes and assayed their ability to induce additional cell divisions. In representative lines from each variant (21), the ability to promote excess asymmetric cell division increased as more sites were eliminated (Fig. 3 and fig. S4). These results strongly suggest that multiple P-X-S/T-P sites are biologically important sites for SPCH regulation. Using mass spectrometry, we found evidence of phosphorylation at several of these functionally critical sites (fig. S5).

Elimination of MAPK target sites generated SPCH variants with greater activity, consistent with phosphorylation of the MPKTD having a repressive role. If the MPKTD is solely a negative regulatory domain, then each of the variants

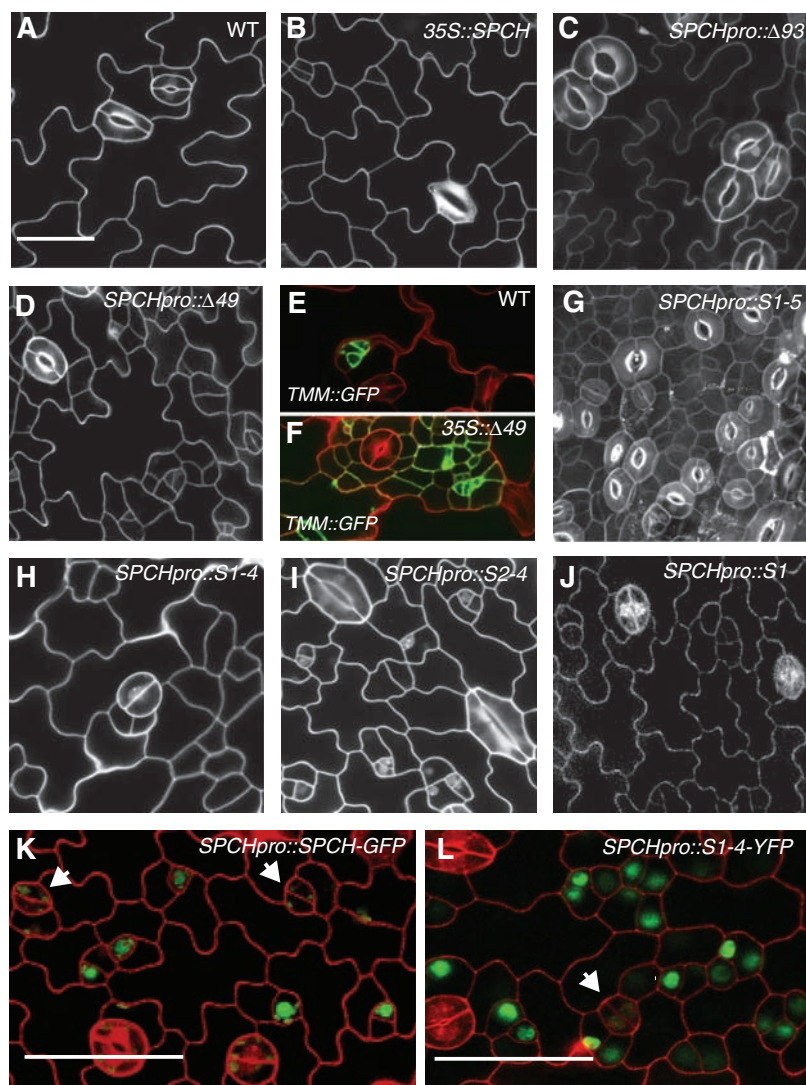


Fig. 2. Confocal images of phenotypes of SPCH variants expressed in plants. (A to D and G to J) Confocal images of 7-dpg abaxial cotyledons. Specific genotypes are noted in upper right corner of images. (E and F) Expression of *TMM*_{pro}::*TMM*-GFP (green) in 35S::SPCHΔ49 (F) compared to wild-type (WT) control (E). (K and L) Comparison of expression pattern for full-length SPCH (K) and SPCH variant with four S/T → A substitutions (L) in abaxial leaves 1 and 2 at 11 dpg. SPCH expression in nuclei is shown in green. Note additional SPCH-expressing cells and persistence of SPCH in young guard cells (white arrow) in (L). Images in (A) to (J) are at the same magnification. Scale bars, 50 μm.

should still rescue *spch* mutant phenotypes. We assayed rescue of *spch-3* by MPKTD deletion and S/T → A variants (fig. S6); in the course of this experiment, we found it necessary to refine our criteria for rescue to include not only the production of stomata (the ultimate result of *SPCH* activity) but also the generation of physically asymmetric cell divisions (the immediate consequence of *SPCH* activity), because multiple *SPCH* variants appeared

to separate these two processes. For example, *SPCHpro::SPCH1-4 S/T>A*, *SPCHpro::SPCHΔ49*, and *35S::SPCHΔ49* did not produce stomata but did induce additional asymmetric divisions (figs. S4I and S6). It was possible to trace the failure to rescue *spch* to a single mutation (Ser¹⁹³ → Ala in *SPCHpro::SPCH1 S>A*) (fig. S6), indicating a positive role for phosphorylation in the MPKTD in addition to negative regulatory elements.

Fig. 3. Production of divisions and stomata by *SPCH* variants in the wild type. Shown are average numbers of stomata and nonstomatal cells (pavement, meristemoid, and small dividing cells) in 0.25-mm² sections of 7-dpg abaxial Col cotyledons expressing the indicated *SPCH* variant with the *SPCH* promoter. Asterisk indicates significant difference from *SPCHpro::SPCH* phenotype [joint confidence coefficient *P* = 99% (21)]. Error bars are ±SE.

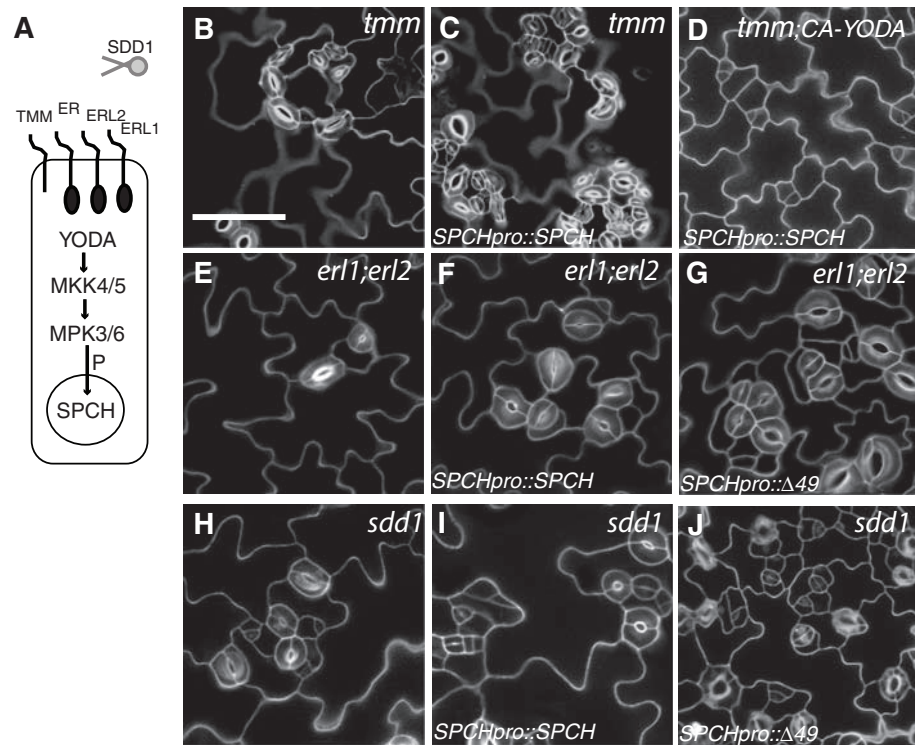
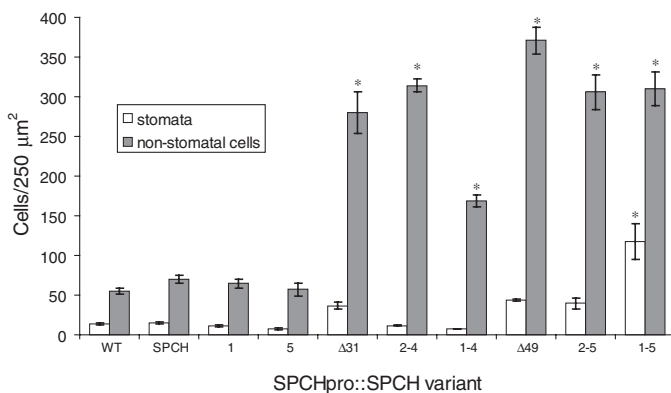


Fig. 4. Effects of endogenous stomatal regulators on *SPCH* function. (A) Scheme of known stomatal regulatory pathway (P, phosphorylation). (B to D) Suppression of *tmm-1*-mediated enhancement of *SPCHpro::SPCH* phenotypes by *CA-YODA*. (B) Baseline of *tmm-1* clustered stomata. (C) Enhanced clusters in *SPCHpro::SPCH; tmm-1*. (D) Block in excess stomatal production by *CA-YODA* in *SPCHpro::SPCH; tmm-1*. (E to G) Enhancement of *SPCH* activity in *erl1;erl2* mutant background. (E) *erl1;erl2* with no stomatal clusters, (F) *SPCHpro::SPCH; erl1;erl2*, and (G) *SPCHpro::SPCHΔ49; erl1;erl2* all result in a statistically significant increase in the stomatal density and fraction of stomata in clusters. (H to J) Lack of enhancement of *SPCH* by *sdd1*. (H) *sdd1* mutants exhibit pairing of stomata and increased density. Expression of *SPCHpro::SPCH* (I) or *SPCHpro::SPCHΔ49* (J) in *sdd1* does not enhance the *sdd1* stomatal overproduction phenotype.

Results with the S/T → A *SPCH* variants suggested that negative regulation by phosphorylation can be a mode of *SPCH* regulation. If the known stomatal regulators and MAPK components are endogenous regulators, then *SPCH* activity should be enhanced when these regulators are eliminated by mutation. Our results support this hypothesis; *SPCHpro::SPCH-GFP* expression in a *tmm-1* background yielded a massive overproduction of stomata instead of a subtle increase in epidermal cell divisions (2) (Fig. 4, B and C). This stomatal overproliferation phenotype could be suppressed by expressing *CA-YODA* in *SPCHpro::SPCH-GFP;tmm-1* plants (Fig. 4D). We further tested the effects of known stomatal regulators on *SPCH* behavior by expressing *SPCHpro::SPCH* and *SPCHpro::SPCHΔ49* in backgrounds with mutations in either *MPK3* or *MPK6* and in a double mutant of the putative upstream receptor-like kinases *ERL1* and *ERL2*. These backgrounds were specifically chosen because none has a stomatal patterning defect on its own (10, 22). In each MAPK and receptor mutant background, the phenotypic effect of *SPCH* expression was significantly enhanced relative to the wild type, consistent with these proteins being endogenous upstream regulators (Fig. 4, E to G, and fig. S7). As a control for whether the effect on *SPCH* activity was specific to MAPK-related stomatal regulators, we also expressed the variants in *sdd1*. *SDD1* is also a negative regulator of stomatal development but was recently shown to act independently of *YODA*, *TMM*, and *ER* in perception of *EPF1* (8). There was no statistically significant increase in stomatal production or clustering when *SPCHpro::SPCH* or *SPCHpro::SPCHΔ49* were expressed in *sdd1* (Fig. 4, H to J, and fig. S7, A and B). Taken together, the behavior of *SPCH* in these mutant backgrounds suggests that members of the established stomatal receptor/MAPK signaling system modulate *SPCH* activity in vivo. These results do not rule out additional regulators or MAPK pathway members being involved in *SPCH* regulation. Furthermore, although these results are consistent with *TMM*, *ER*-family receptors, and the MAPKs controlling *SPCH* activity itself, it is also possible that these proteins regulate the behavior of cells produced by *SPCH* activity.

Eliminating MAPK target sites affects *SPCH* function and subsequent stomatal development; however, these experiments do not address the mechanism by which phosphorylation affects *SPCH*. Substrates of MAPK phosphorylation are often associated with changes in localization, stability, or interaction partners (23, 24). All *SPCH* variants are constitutively nuclear (2) (Fig. 2, K and L), which suggests that *SPCH* phosphorylation does not alter its subcellular localization; however, it is possible that *SPCH* phosphorylation alters *SPCH* persistence. A structural hint of this mechanism is the presence of a predicted PEST domain [PESTfind score +7.63 (21)] in the *SPCH* MPKTD (fig. S5). Functionally, elimination of MPKTD phosphorylation sites results in excess *SPCH* protein as visualized by YFP expression.

Typically, early in leaf development, *SPCHpro::SPCH-YFP* is expressed in many small cells, but fluorescence diminishes as cells become morphologically distinct meristemoids (2) (Fig. 2K). Relative to equivalently staged *SPCHpro::SPCH-YFP* plants, *SPCH* variants with strong overproliferation phenotypes displayed increased numbers of YFP-positive cells early (Fig. 2L) and a trend toward increased protein persistence into meristemoid, GMC, and guard cell stages later (Fig. 2L and fig. S8). When expressed in a *CA-YODA* background (in which *SPCH* was predicted to be phosphorylated), full-length *SPCH-GFP* was not visible, nor could it promote stomatal development (figs. S2 and S9C). However, GFP-*SPCHΔ49*, which is missing phosphorylatable residues, was detectable and was able to drive asymmetric divisions (fig. S9D).

SPCH is closely related to two other bHLH transcription factors that control stomatal development. We have shown, however, that a novel domain of *SPCH* renders it uniquely subject to phospho-regulation by a group of kinases that have been demonstrated to transduce signals downstream of both cell-cell and plant-environment interactions (fig. S10). In general, the domain mediates repression of *SPCH* and does so in a quantitative manner; the more potential MAPK sites eliminated, the stronger the effect of the *SPCH* variant on stomatal development. However, one specific residue phosphorylated by MPK6, Ser¹⁹³, is required positively for activity, which suggests that the MPKTD is the integration site for complex regulatory inputs. The MPKTD is of unknown origin; it is not present in *Arabidopsis* proteins other than *SPCH* but is found in *SPCH*

homologs from a variety of plant species (fig. S11) (25), hence MAPK regulation of a stomatal bHLH is likely to be a widespread regulatory strategy.

SPCH solves a problem intrinsic to MAPK signaling—how is a set of generally used MAPKs recruited to a specific biological event?—by providing the important effector in a spatially and temporally restricted domain. From the perspective of stomatal control, *SPCH* guards the entry into the stomatal lineage, including the production of self-renewing cells that contribute to later flexibility in epidermal development. This important decision point is likely the target of developmental, physiological, and environmental regulation (26, 27). Coupling the MPK3/6 signaling module to the activity of *SPCH* provides a unified, yet tunable, output for the complex set of inputs from these sources. Understanding the elements of the MAPK/*SPCH* regulatory system that coordinate stomatal production with the prevailing climate may allow the production of food or bioenergy crops with the ability to respond and adapt to changes in that climate.

References and Notes

1. K. Ohashi-Ito, D. Bergmann, *Plant Cell* **18**, 2493 (2006).
2. C. A. MacAlister, K. Ohashi-Ito, D. Bergmann, *Nature* **445**, 537 (2007).
3. L. J. Pillitteri, D. Sloan, N. Bogenschutz, K. Torii, *Nature* **445**, 501 (2007).
4. M. M. Kanaoka *et al.*, *Plant Cell* **20**, 1775 (2008).
5. E. D. Shpak, J. M. McAbee, L. J. Pillitteri, K. U. Torii, *Science* **309**, 290 (2005).
6. J. Masle, S. Gilmore, G. Farquhar, *Nature* **436**, 866 (2005).
7. J. A. Nadeau, F. D. Sack, *Science* **296**, 1697 (2002).
8. K. Hara, R. Kajita, K. Torii, D. Bergmann, T. Kakimoto, *Genes Dev.* **21**, 1720 (2007).
9. D. Berger, T. Altmann, *Genes Dev.* **14**, 1119 (2000).

10. H. Wang, N. Ngwenyama, Y. Liu, J. Walker, S. Zhang, *Plant Cell* **19**, 63 (2007).
11. D. C. Bergmann, W. Lukowitz, C. R. Somerville, *Science* **304**, 1494 (2004).
12. C. Jonak, L. Okresz, L. Bogre, H. Hirt, *Curr. Opin. Plant Biol.* **5**, 415 (2002).
13. M. Karin, *Ann. N.Y. Acad. Sci.* **851**, 139 (1998).
14. H. Wang *et al.*, *Plant Cell* **20**, 602 (2008).
15. W. Lukowitz, A. Roeder, D. Parmenter, C. Somerville, *Cell* **116**, 109 (2004).
16. T. Asai *et al.*, *Nature* **415**, 977 (2002).
17. Y. Kovtun, W. Chiu, G. Tena, J. Sheen, *Proc. Natl. Acad. Sci. U.S.A.* **97**, 2940 (2000).
18. J.-X. He, J. Gendron, Y. Yang, J. Li, Z. Wang, *Proc. Natl. Acad. Sci. U.S.A.* **99**, 10185 (2002).
19. T. L. Tootle, I. Rebay, *Bioessays* **27**, 285 (2005).
20. C. Widmann, S. Gibson, M. Jarpe, G. Johnson, *Physiol. Rev.* **79**, 143 (1999).
21. See supporting material on Science Online.
22. E. D. Shpak, M. Lakeman, K. Torii, *Plant Cell* **15**, 1095 (2003).
23. S. Joo, Y. Liu, A. Lueth, S. Zhang, *Plant J.* **54**, 129 (2008).
24. M. Ebisuya, K. Kondoh, E. Nishida, *J. Cell Sci.* **118**, 2997 (2005).
25. X. Li *et al.*, *Plant Physiol.* **141**, 1167 (2006).
26. D. Bergmann, F. Sack, *Annu. Rev. Plant Biol.* **58**, 63 (2007).
27. A. M. Hetherington, F. Woodward, *Nature* **424**, 901 (2003).
28. We thank lab members for discussion and comments on the manuscript, The Carnegie Department of Plant Biology for use of microscopes, and L. Smith for identification of maize homologs. Supported by NSF grant IOS-0544895, U.S. Department of Energy grant DE-FG02-06ER15810, a Terman award, and the Stanford Genome Training Program (National Human Genome Research Institute).

Supporting Online Material

www.sciencemag.org/cgi/content/full/322/5904/1113/DC1
Materials and Methods

SOM Text

Figs. S1 to S11

References

24 June 2008; accepted 14 October 2008

10.1126/science.1162263

Regulatory Genes Control a Key Morphological and Ecological Trait Transferred Between Species

Minsung Kim,^{1,3*} Min-Long Cui,^{1*} Pilar Cubas,^{1,4*} Amanda Gillies,² Karen Lee,¹ Mark A. Chapman,^{2,5} Richard J. Abbott,² Enrico Coen^{1†}

Hybridization between species can lead to introgression of genes from one species to another, providing a potential mechanism for preserving and recombining key traits during evolution. To determine the molecular basis of such transfers, we analyzed a natural polymorphism for flower-head development in *Senecio*. We show that the polymorphism arose by introgression of a cluster of regulatory genes, the *RAY* locus, from the diploid species *S. squalidus* into the tetraploid *S. vulgaris*. The *RAY* genes are expressed in the peripheral regions of the inflorescence meristem, where they promote flower asymmetry and lead to an increase in the rate of outcrossing. Our results highlight how key morphological and ecological traits controlled by regulatory genes may be gained, lost, and regained during evolution.

Changes in regulatory genes have been implicated in a range of evolutionary transitions, operating from the micro- to macro-evolutionary scales (1–3). These changes have largely been considered as occurring independently within different species. However, it is

also possible that interspecific hybridization plays an important role in evolution (4). One consequence of such exchanges is that they may allow traits that are lost because of short-term selective pressures to be regained at a later stage. For example, members of the sunflower family (Asteraceae)

share a composite flower head, with each head comprising numerous small flowers (florets). In radiate species, the outer florets (ray florets) have large attractive petals, whereas the inner florets (disc florets) tend to be less conspicuous. Loss of the radiate condition has occurred multiple times within the Asteraceae, yielding nonradiate species with only disc florets (5). These events often correlate with shifts to higher levels of self-pollination (6), which should be favored when mates and/or pollinators occur at low densities (7). Partial or complete reversals from the nonradiate back to the radiate condition have been described (8), some of which appear to involve interspecific hybridization events (9). One explanation for such evolutionary gains and losses is that key regulatory genes control-

¹Department of Cell and Developmental Biology, John Innes Centre, Colney Lane, Norwich NR4 7UH, UK. ²School of Biology, University of St. Andrews, St. Andrews KY16 9TH, UK. ³Faculty of Life Sciences, University of Manchester, Manchester M13 9PT, UK. ⁴Centro Nacional de Biotecnología/CSIC, Darwin 3, Campus UAM, 28049 Madrid, Spain. ⁵Department of Plant Biology, University of Georgia, Athens, GA 30602, USA.

*These authors contributed equally to this work.

†To whom correspondence should be addressed. E-mail: enrico.coen@bbsrc.ac.uk.

***Arabidopsis* Stomatal Initiation Is Controlled by MAPK-Mediated Regulation of the bHLH SPEECHLESS**

Gregory R. Lampard, Cora A. MacAlister and Dominique C. Bergmann

Science **322** (5904), 1113-1116.
DOI: 10.1126/science.1162263

ARTICLE TOOLS

<http://science.sciencemag.org/content/322/5904/1113>

SUPPLEMENTARY MATERIALS

<http://science.sciencemag.org/content/suppl/2008/11/13/322.5904.1113.DC1>

RELATED CONTENT

<http://stke.sciencemag.org/content/sigtrans/1/46/ec398.abstract>

REFERENCES

This article cites 26 articles, 14 of which you can access for free
<http://science.sciencemag.org/content/322/5904/1113#BIBL>

PERMISSIONS

<http://www.sciencemag.org/help/reprints-and-permissions>

Use of this article is subject to the [Terms of Service](#)